SHOCKS AND NONTHERMAL PROCESSES IN CLUSTERS

CRAIG L. SARAZIN

Department of Astronomy, University of Virginia, P. O. Box 3818,
Charlottesville, VA 22903-0818, U.S.A.

Clusters of galaxies generally form by the gravitational merger of smaller clusters and groups. Major cluster mergers are the most energetic events in the Universe since the Big Bang. Mergers drive shocks into the intracluster gas, and these shocks heat the intracluster gas, and should also accelerate nonthermal relativistic particles. The X-ray signatures of the thermal effects of merger shocks will be discussed. X-ray observations of shocks can be used to determine the geometry and kinematics of the merger. As a result of particle acceleration in shocks, clusters of galaxies should contain very large populations of relativistic electrons and ions. Electrons with Lorentz factors $\gamma \sim 300$ (energies $E = \gamma m_e c^2 \sim 150$ MeV) are expected to be particularly common. Observations and models for the radio, extreme ultraviolet, hard X-ray, and gamma-ray emission from nonthermal particles accelerated in these shocks will also be described. The predicted gamma-ray fluxes of clusters should make them easily observable with GLAST.

1 Introduction

Major cluster mergers are the most energetic events in the Universe since the Big Bang. Cluster mergers are the mechanism by which clusters are assembled. In these mergers, the subclusters collide at velocities of $\sim$2000 km/s, and shocks are driven into the intracluster medium. In major mergers, these hydrodynamical shocks dissipate energies of $\sim 3 \times 10^{63}$ ergs; such shocks are the major heating source for the X-ray emitting intracluster medium. The shock velocities in merger shocks are similar to those in supernova remnants in our Galaxy, and we expect them to produce similar effects. Mergers shocks should heat and compress the X-ray emitting intracluster gas, and increase its entropy. We also expect that particle acceleration by these shocks will produce nonthermal electrons and ions, and these can produce synchrotron radio, inverse Compton (IC) EUV and hard X-ray, and gamma-ray emission.

Hydrodynamical simulations of cluster formation and evolution have shown the importance of merger shocks.[45,39] The evolution of the structure of merger shocks is illustrated in Figure 1,[37] which shows an off-center merger between two symmetric subclusters. At early stages in the merger (prior to the first panel), the shocked region is located between the two subcluster centers and is bounded on either side by two shocks. At this time, the subcluster centers, which may contain cooling cores and central radio sources, are not affected. Later, these shocks sweep over the subcluster centers (the first panel); the survival of central cool cores depends on how sharply peaked the potentials of the subclusters are.[31,37] The main merger shocks pass into the outer parts of the merging system (panel 2), and secondary shocks may appear in the inner regions
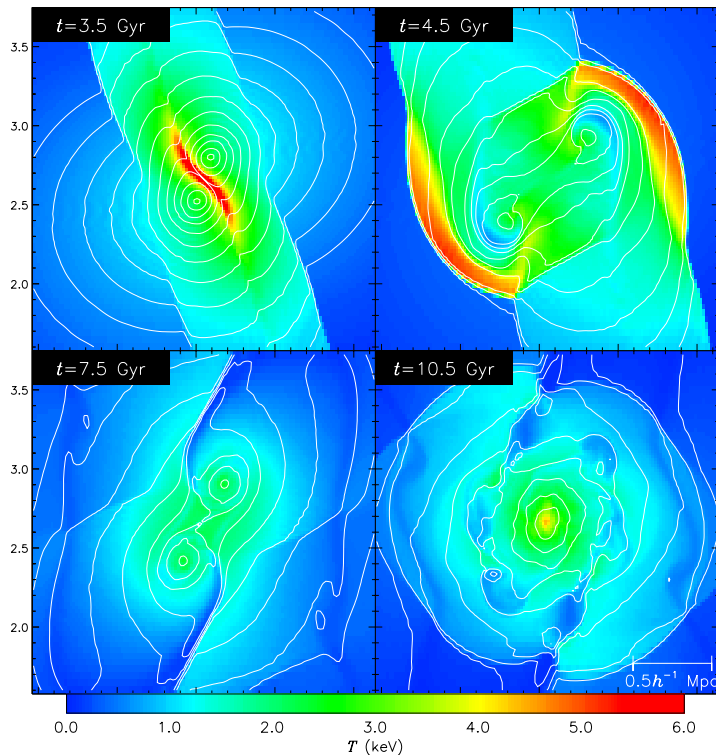
Figure 1: The results of a hydro simulation of a symmetric, off-center merger by Ricker and Sarazin.[37] The colors show the temperature, while the contours are the X-ray surface brightness. Initially, the shocked region is located between the two subcluster centers. Later, the main merger shocks propogate to the outer parts of the cluster, and other weaker shocks also occur. By the end of the simulation, the cluster is beginning to return to equilibrium.

(panel 3). Eventually, the cluster begins to return to equilibrium (panel 4).

2   Thermal Effects of Merger Shocks

2.1   Shock Kinematics

Merger shocks heat and compress the intracluster gas, and these effects can be used to determine the geometry and kinematics of the merger. ASCA X-ray temperature maps and ROSAT images have been used in an initial effort to apply this technique.[31] The cluster containing the radio source Cygnus A is a particularly simple case (Fig. 2). This appears to be a fairly symmetric merger with a low impact parameter. The merger is at an early phase, with the merger shocks being located between the two subcluster centers. A hydro/N-body simulation of the merger[37] is shown at the right in Fig. 2 (not to the same scale). Presumably, the fact that the merger shocks have not yet passed through the subcluster centers is the reason why the merger hasn't disrupted the Cygnus A radio source or the surrounding cooling flow.

The simple geometry of this merger makes it easy to apply the shock jump conditions to determine the merger velocity. From the Rankine–Hugoniot jump conditions, the velocity change across the merger shock is

$$\Delta u_{sh} = \left[\frac{kT_0}{\mu m_p} \left(r - 1 \right) \left(\frac{T_1}{T_0} - \frac{1}{r} \right) \right]^{1/2}, \tag{1}$$

where T_0 and T_1 are the pre- and post-shock temperature, μ is the mean mass per particle, and
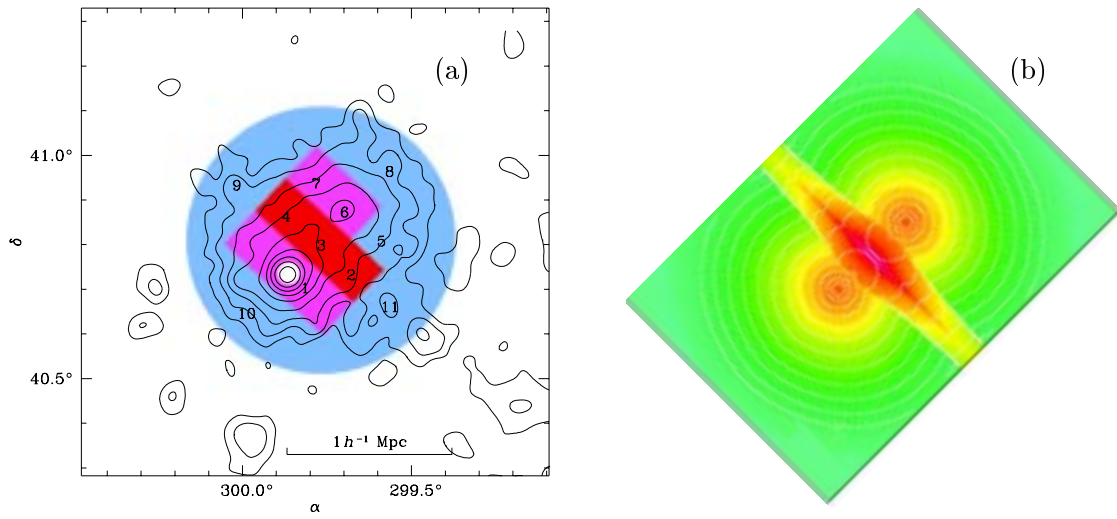
Figure 2: (a) ROSAT PSPC contours of the Cygnus A cluster. The radio galaxy is located at the center of the cooling flow peak in the southeast subcluster. A second subcluster is centered on the X-ray peak $11'$ to the northwest (labeled 6). The color shows the ASCA temperatures (red being hot, blue being cool), and indicates that a merger shock region is located between the two subcluster centers.[31] (b) A hydro/N-body simulation of the Cygnus A cluster merger,[37] not to the same scale as panel (a) but rotated to the same orientation.

the shock compression r is given by

$$\frac{1}{r} = \left[\frac{1}{4} \left(\frac{\gamma + 1}{\gamma - 1} \right)^2 \left(\frac{T_1}{T_0} - 1 \right)^2 + \frac{T_1}{T_0} \right]^{1/2} - \frac{1}{2} \frac{\gamma + 1}{\gamma - 1} \left(\frac{T_1}{T_0} - 1 \right). \tag{2}$$

For a symmetric merger, the merger velocity of the two subclusters is just $\Delta u_{cl} = 2\Delta u_{sh}$. When the ASCA temperatures are used, this gives $\Delta u_{cl} \approx 2200$ km/s. The radial velocity distribution of the galaxies in this cluster is bimodal,[34] and consistent with a merger velocity of 2400 km/s.

Interestingly, the collision velocity found above is close to the free-fall velocity of $\sim$2200 km/s that the two subclusters should have achieved had they fallen from a large distance to their observed separation. This consistency suggests that the shock energy is effectively thermalized, and that a major fraction does not go into turbulence, magnetic fields, or cosmic rays.

2.2   Nonequilibrium Effects

Cluster merger are expected to produce collisionless shocks, as occurs in supernova remnants. As such, nonequilibrium effects are expected, including nonequipartition of electrons and ions and nonequilibrium ionization.[31,48] In fact, observations of a central shock in the spectacular merging cluster Abell 3667 show an apparent lag of $\sim$200 kpc between the shock position and the peak in the electron temperature.[31] This is consistent with weak electron heating at the shock, and the timescale for Coulomb heating. However, recent Chandra observations of this cluster suggest a more complex situation.[50]

2.3   Early Chandra Results

Although ASCA and ROSAT observations provide some evidence for merger shocks, they lack the combination of spatial and spectral resolution over a hard X-ray band needed to really determine shock structures accurately. Chandra has superb spatial resolution, while XMM has a wider field of view and a very large collecting area. Astro-E would have provided very high spectral resolution, sufficient to directly detect the Doppler motions in the gas. Hopefully, an equivalent capability will be provided in the not too distant future.
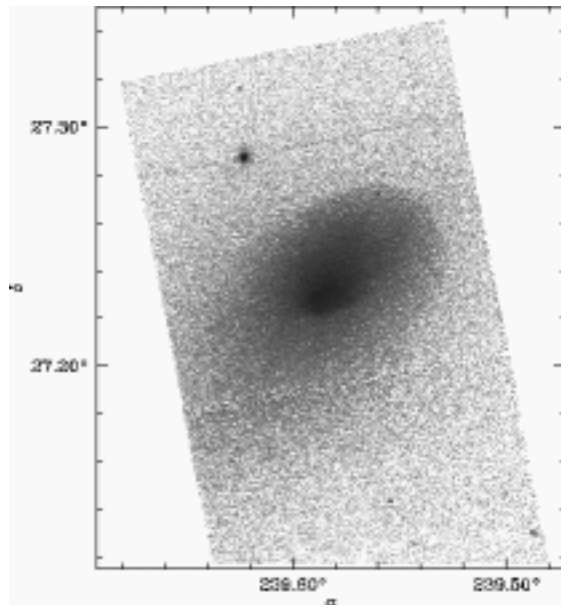
Figure 3: The Chandra X-ray image of the central region of the merging cluster Abell 2142 from Markevitch et al.[32] Note the two bow-shaped discontinuities to the northwest and just south of the brightest region of the cluster.

A number of merging clusters were included in the early observations with Chandra taken for calibration and science verification purposes, and several of these have shown sharp structures which initially appeared to be shocks. An example is Abell 2142 (Fig. 3), for which a careful analysis has been given by Markevitch et al.[32] Even the raw Chandra image shows two bow-shaped structures, to the south and northwest of the center. However, the Chandra spectra show that these are not shocks. As one moves inward and the gas density increases abruptly, the gas temperature decreases in such a way that the pressure is fairly continuous. Thus, the specific entropy is actually lower in the denser "shocked" region than in the lower density "pre-shock" region. These are not shocks, but rather contact discontinuities between higher density cool gas and lower density hot gas. Markevitch et al.[32] argue that the merger shocks have already passed though the lower density gas in these regions, and that the denser cooler gas regions are the remnants of the cooling cores of the original subclusters, which are now plowing through the lower density shocked gas. A very similar situation has been found in Abell 3667.[50]

3 Particle Acceleration and Nonthermal Emission

3.1 Shock Acceleration

Radio observations of supernova remnants indicate that shocks with $v \gtrsim 10^3$ km/s convert at least a few percent of the shock energy into the acceleration of relativistic electrons.[10] Even more energy may go into relativistic ions. While the merger shocks in cluster have lower Mach numbers and compressions than the blast waves in young supernova remnants, it is probable that shock acceleration operates efficiently in clusters as well. Given that all of the thermal energy of the intracluster gas in clusters is due to shocks with such velocities, it seems likely that relativistic electrons with a total energy of $\gtrsim 10^{62}$ ergs are produced in clusters, with perhaps even higher energies in ions.

Clusters are also very good storage locations for cosmic rays. Under reasonable assumptions for the diffusion coefficient, particles with energies $\lesssim 10^6$ GeV have diffusion times which are longer than the Hubble time.[2,11] Figure 4 gives the loss time scales for relativistic electrons under typical intracluster conditions. Although high energy electrons lose energy rapidly due to
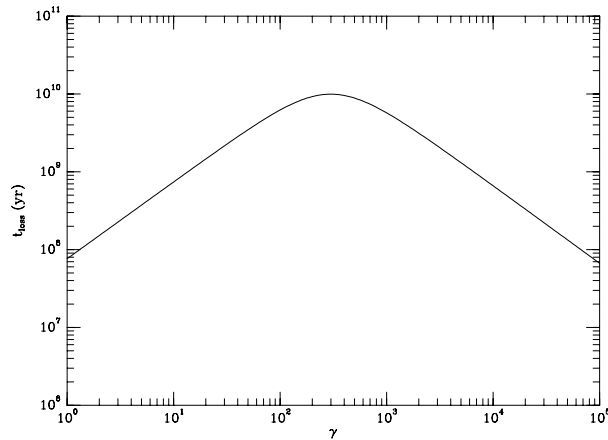
Figure 4: The loss time scale for relativistic electrons in a cluster of galaxies under typical intracluster conditions as a function of their Lorentz factor γ. The particles have energies of $E = \gamma m_e c^2$.

IC and synchrotron emission, electrons with Lorentz factors of $\gamma \sim 300$ (energies ~ 150 MeV) have long lifetimes which approach the Hubble time.[41,44] Thus, clusters of galaxies can retain low energy electrons ($\gamma \sim 300$) and nearly all cosmic ray ions for a significant fraction of a Hubble time.

Recently, I have calculated models for the relativistic electrons in clusters, assuming they are primary electrons accelerated in merger shocks.[41,42] An alternative theory is that these particles are secondaries produced by the decay of charged mesons generated in cosmic ray ion collisions.[11] Two recent cluster merger simulations have included particle acceleration approximately.[38,49] Their conclusions are very similar to mine based on simpler models. The populations of cosmic ray electrons in clusters depends on their merger histories. Because low energy electrons have long lifetimes, one expects to find a large population of them in most clusters (any cluster which has had a significant merger since $z \sim 1$). On the other hand, higher energy electrons ($E \gtrsim 1$ GeV) have short lifetimes (shorter than the time for a merger shock to cross a cluster). Thus, one only expects to find large numbers of higher energy electrons in clusters which are having or have just had a merger.

Fig. 5(a) shows the electron spectrum in a cluster with a typical history. Most of the electron energy is in electrons with $\gamma \sim 300$, which have the longest lifetimes. These electrons are produced by mergers over the entire history of the cluster. This cluster also has a small ongoing merger which produces the high energy tail on the electron distribution.

Most of the emission from these electrons is due to IC, and the resulting spectrum is shown in Fig. 5(b). For comparison, thermal bremsstrahlung with a typical rich cluster temperature and luminosity is shown as a dashed curve. Fig. 5(b) shows that clusters should be strong sources of extreme ultraviolet (EUV) radiation. Since this emission is due to electrons with $\gamma \sim 300$ which have very long lifetimes, EUV radiation should be a common feature of clusters.[44]

In clusters with an ongoing merger, the higher energy electrons will produce a hard X-ray tail via IC scattering of the Cosmic Microwave Background (CMB); the same electrons will produce diffuse radio synchrotron emission.

3.2 EUV/Soft X-ray Emission

Excess EUV emission has apparently been detected with the EUVE satellite in six clusters (Virgo, Coma, Abell 1795, Abell 2199, Abell 4038, & Abell 4059).[27,28,8,33,9,22,29,30,3,6,7] In fact, the EUVE satellite appears to have detected all of the clusters it observed which are nearby, which have long integration times, and which lie in directions of low Galactic column where detection is possible at these energies. However, the EUV detections and claimed properties of
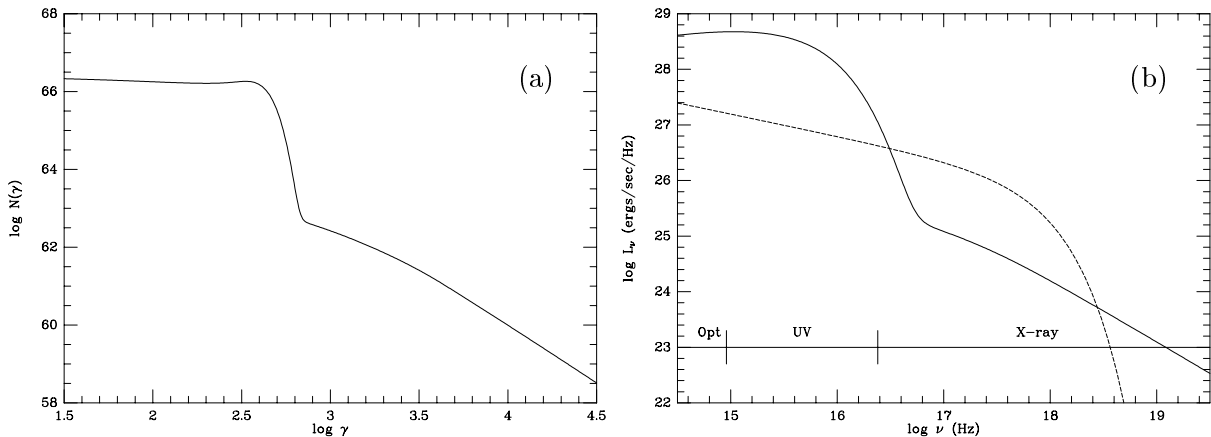
Figure 5: (a) A typical model for the relativistic electron population in a cluster of galaxies. The lower energy electrons are due to all of the mergers in the cluster history, while the high energy electrons are due to a small current merger. (b) The IC spectrum from the same model (solid curve). The dashed curve is a 7 keV thermal bremsstrahlung spectrum.

the clusters remain quite controversial.[8,1,9,3]

The EUV observations suggest that rich clusters generally have EUV luminosities of $\sim 10^{44}$ ergs/s, and have spectra which decline rapidly in going from the EUV to the X-ray band. The EUV emission is very spatially extended. The last point is illustrated in Figure 6. The data points show the ratio of the EUV to thermal X-ray emission in the cluster Abell 1795. The ratio increases rapidly with increasing radius.

While it is possible that the EUV emission may be thermal in origin,[14,6] I believe that it is more likely that this emission is due to inverse Compton scattering (IC) of CMB photons by low energy relativistic electrons.[21,8,13,44] In this model, the EUV would be produced by electrons with energies of ~ 150 MeV ($\gamma \sim 300$; Fig. 5). As noted above, these electrons have lifetimes which are comparable to the Hubble time, and should be present in essentially all clusters. This can explain why EUV emission is common. To produce the EUV luminosities observed, one needs a population of such electrons with a total energy of $\sim 10^{62}$ ergs, which is about 3% of the typical thermal energy content of clusters. This is a reasonable acceleration efficiency for these particles, given that both the thermal energy in the intracluster gas and the relativistic particles result from merger shocks. The steep spectrum in going from EUV to X-ray bands is predicted by this model [Fig. 5(b)], it results from the rapid increase in losses ($\propto \gamma^2$) for particles as the energy increases above $\gamma \sim 300$ (Fig. 4).

The broad spatial distribution of the EUV is also naturally explained by the density dependence of IC emission. The thermal emission which produces the bulk of the X-ray emission in clusters is due to collisions between thermal electrons and ions; thus, it declines with the square of the density as the radius increases. On the other hand, IC emission is due to collisions between cosmic ray electrons and CMB photons; since the CMB energy density is extremely uniform, IC EUV emission varies with a single power of density, rather than density squared. This simple difference can explain why the EUV is more extended than the thermal X-ray emission. As a example, the solid curve in Figure 6 shows the predicted ratio of EUV to X-ray emission in Abell 1795, if the pressure in cosmic ray electrons varies in proportion with the thermal gas pressure, and the latter is determined from the X-ray observations.[44]

3.3 Hard X-ray Tails

If clusters contain higher energy relativistic electrons with $\gamma \sim 10^4$, these particles will produce hard X-ray emission by IC scattering, and radio synchrotron emission depending on the intracluster magnetic field. Since these higher energy electrons have short lifetimes, they should only
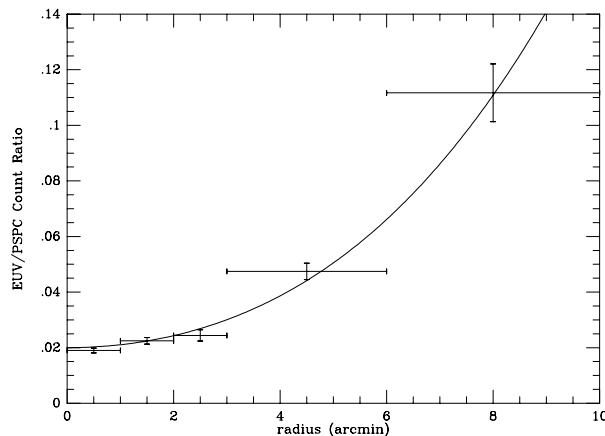
Figure 6: The data points give the observed ratio of the EUV to thermal X-ray surface brightness versus radius in the cluster Abell 1795 from Mittaz et al.[33] The EUV data is from EUVE, while the X-ray data is from the ROSAT PSPC. The solid curve is the IC model from Sarazin & Lieu,[44] assuming that the pressure in cosmic ray electrons in this cluster varies in proportion with the thermal pressure in the X-ray emitting gas, as determined with the ROSAT PSPC.

be present in clusters with evidence for a recent or ongoing merger.

Hard X-ray emission in excess of the thermal emission and detected as a nonthermal tail at energies $\gtrsim$20 keV has been seen in at least two clusters. The Coma cluster, which is undergoing at least one merger and which has a radio halo, was detected with both BeppoSAX and RXTE.[17,36] BeppoSAX also has detected Abell 2256,[18] another merger cluster with strong diffuse radio emission. BeppoSAX may have detected Abell 2199,[22] although I believe the evidence is less compelling for this case. A nonthermal hard X-ray detection of Abell 2199 would be surprising, as this cluster is very relaxed and has no radio halo or relic.[24] An alternative explanation of the hard X-ray tails is that they might be due to nonthermal bremsstrahlung,[43] which is bremsstrahlung from nonthermal electrons with energies of 10–1000 keV which are being accelerated to higher energies.

3.4 Radio Halos and Relics

A number of clusters of galaxies are known to contain large-scale diffuse radio sources which have no obvious connection to individual galaxies in the cluster.[19] These sources are referred to as radio halos when they appear projected on the center of the cluster, and are called relics when they are found on the cluster periphery. The best known and studied radio halo is in the Coma cluster.[12] These radio halos and relics are relatively uncommon; about 40 are known at the present time. They are diffuse radio sources with very steeply declining radio spectra. In all cases of which I am aware, they have been found in clusters which show significant evidence for an ungoing merger.[19,15,16] This suggests that the relativistic electrons are accelerated by merger shocks. In the early stages of mergers, halos are often found on the border between the subclusters, where the cluster gas is first being shocked (e.g., Abell 85).[46] In more advanced mergers, more conventional centrally located halos (e.g., Coma) and peripheral relics (e.g., Abell 3667) are found. Abell 3667 provides a spectacular case of two bow-shaped radio relics at opposite sides of a merging cluster,[40] and located at the positions where merger shocks are predicted.[38]

Although radio halos and relics have been studied for some time, lately the number of known cases has increased dramatically. This is largely due to the radio surveys (like NVSS and WENSS) and new low frequency radio instruments. Perhaps the largest number of new sources have come from the NVSS survey and VLA pointed observation follow up effort by Giovannini, Feretti, and collaborators.[19] Other new detections have involved other VLA surveys,[35] the VLA at 74 MHz,[23] SUMSS and MOST,[40] the ATCA,[26] and WENSS.[25]
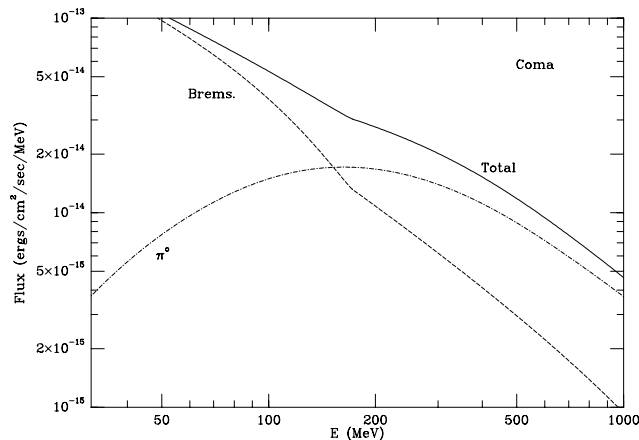
Figure 7: The predicted gamma-ray spectrum for the Coma cluster, including electron bremsstrahlung and π^o decay from ions.[42]

3.5 Predicted Gamma-Ray Emission

Relativistic electrons and ions in clusters are also expected to produce strong gamma-ray emission.[11,5,4,42] The region near 100 MeV is particularly interesting, as this region includes bremsstrahlung from the most common electrons with $\gamma \sim 300$, and gamma-rays from ions produced by π^o decay. Both of these processes involve collisions between relativistic particles (electrons for bremsstrahlung, ions for π^o emission) and thermal particles, so they should both vary in the same way with density in the cluster. Thus, the ratio of these two spectrally distinguishable emission processes should tell us the ratio of cosmic ray ions to electrons in clusters.[4,42]

Figure 7 shows the predicted gamma-ray spectrum for the Coma cluster, based on a model which reproduces the observed EUV, hard X-ray, and radio emission.[42] The observed upper limit from CGO/EGRET is $<4 \times 10^{-8}$ cts/cm^2/s for $E > 100$ MeV,[47] while the predicted value for this model is $\sim 2 \times 10^{-8}$ cts/cm^2/s. The EGRET upper limit already shows that the ratio of ions to electrons cannot be too large ($\lesssim 30$).[4,42]) The predicted fluxes are such that many nearby clusters should be easily detectable with GLAST.

References

1. Arabadjis, J. S., & Bregman, J. N. 1999, ApJ, 514, 607
2. Berezinsky, V. S., Blasi, P., & Ptuskin, V. S. 1997, ApJ, 487, 529
3. Berghöfer, T. W., Bowyer, S., & Korpela, E. 2000, ApJ, 535, 615
4. Blasi, P. 1999, ApJ, 525, 603
5. Blasi, P., & Colafrancesco, S. 1999, APh, 12, 169
6. Bonamente, M., Lieu, R., & Mittaz, J. 2000, ApJ, in press

7. Bowyer, S. 2000, private communication

8. Bowyer, S., & Berghöfer, T. W. 1998, ApJ, 506, 502

9. Bowyer, S., Berghöfer, T. W., & Korpela, E. 1999, ApJ, 526, 592

10. Blandford, R. D., & Eichler, D. 1987, Phys. Rep., 154, 1

11. Colafrancesco, S., & Blasi, P. 1998, APh, 9, 227

12. Deiss, B. M., Reich, W., Lesch, H., & Wielebinski, R. 1997, A&A, 321, 55D

13. Enßlin, T. A., & Biermann, P. L. 1998, A&A, 330, 90

14. Fabian, A. C. 1997, Science, 275, 48

15. Feretti, L. 1999, in Proc. Diffuse Thermal and Relativistic Plasma in Galaxy Clusters, ed. H. Böringer, L. Feretti, & P. Schuecker (Garching: MPE), 1

16. Feretti, L. 2000, preprint (astro-ph/0006379)

17. Fusco-Femiano, R., et al., 1999, ApJ, 513, L21

18. Fusco-Femiano, R., et al., 2000, ApJ, 534, L7

19. Giovannini, G., et al., 1993, ApJ, 406, 399

20. Giovannini, G., Tordi, M., & Feretti, L. 1999, New Astronomy, 4, 14

21. Hwang, C.-Y. 1997, Science, 278, 1917

22. Kaastra, J. S., et al., 1999, ApJ, 519, L119

23. Kassim, N. E., Perley, R. A., & Erickson, W. C. 1999, in Proc. Diffuse Thermal and Relativistic Plasma in Galaxy Clusters, ed. H. Böringer, L. Feretti, & P. Schuecker (Garching: MPE), 49

24. Kempner, J., & Sarazin, C. L. 2000a, ApJ, 530, 282

25. Kempner, J., & Sarazin, C. L. 2000b, ApJ, submitted

26. Liang, H., Hunstead, R. W., Birkinshaw, M., & Andreani, P. 2000, ApJ, in press

27. Lieu, R., et al., 1996, Science, 274, 1335

28. Lieu, R., et al., 1996, ApJ, 458, L5

29. Lieu, R., Bonamente, M., & Mittaz, J. 1999, ApJ, 517, L91

30. Lieu, R., et al., 1999, ApJ, 527, L77

31. Markevitch, M., Sarazin, C. L., & Vikhlinin, A. 1999, ApJ, 521, 526

32. Markevitch, M., et al., 2000, ApJ, in press

33. Mittaz, J. P. D., Lieu, R., & Lockman, F. J. 1998, ApJ, 498, L17

34. Owen, F. N., et al., 1997, ApJ, 488, L15

35. Owen, F. N., Morrison, G., & Voges, W. in Proc. Diffuse Thermal and Relativistic Plasma in Galaxy Clusters, ed. H. Böringer, L. Feretti, & P. Schuecker (Garching: MPE), 9

36. Rephaeli, Y., Gruber, D., & Blanco, P. 1999, ApJ, 511, L21

37. Ricker, P. M., & Sarazin, C. L. 2000, preprint

38. Roettiger, K., Burns, J., & Stone, J. M. 1999, ApJ, 518, 603

39. Roettiger, K., Stone, J. M., & Burns, J. 1999, ApJ, 518, 594

40. Röttgering, H., Wieringa, M., Hunstead, R., & Ekers, R. 1997, MNRAS, 290, 57

41. Sarazin, C. L. 1999, ApJ, 520, 529

42. Sarazin, C. L. 2000, preprint

43. Sarazin, C. L., & Kempner, J. 2000, ApJ, in press

44. Sarazin, C. L., & Lieu, R. 1998, ApJ, 494, L177

45. Schindler, S., & Müller E. 1993, A&A, 272, 137

46. Slee, O. B., & Reynolds, J. E. 1984, PASA, 5, 516

47. Sreekumar, P., et al., 1996, ApJ, 464, 628

48. Takizawa, M. 1999, ApJ, 520, 514

49. Takizawa, M., & Naito, T. 2000, ApJ, 535, 586

50. Vikhlinin, A., et al., 2000, preprint